Mitigating uncertainty in inverse wave scattering

Liliana Borcea
Mathematics
University of Michigan, Ann Arbor,

Inverse wave scattering problem

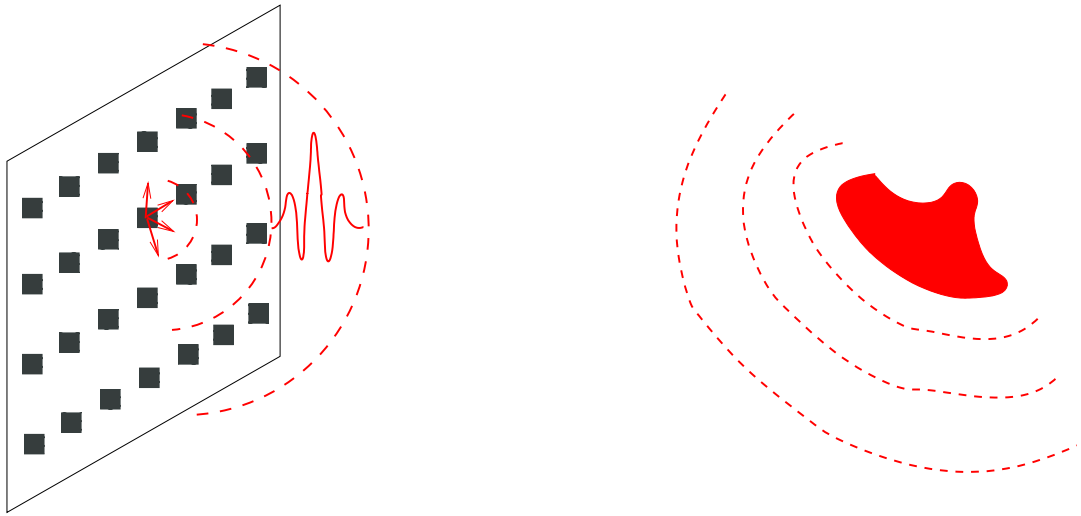

Generic setup: A collection (array) of sensors probes a medium with signals (pulses, chirps) that generate waves which are scattered by inhomogeneities. The sensors collect the scattered waves and the goal of the inversion is to estimate the medium.

Numerous applications: medical ultrasound, nondestructive avaluation of structures, radar imaging, oil exploration, etc.

Inverse problem for wave equations

- **Sound waves:** pressure $p(t,\vec{x})$ and velocity $\vec{v}(t,\vec{x})$ satisfy

$$\frac{\sigma(\vec{x})}{c(\vec{x})}\partial_t\vec{v}(t,\vec{x}) + \nabla p(t,\vec{x}) = \vec{F}(t,\vec{x})$$
$$\partial_t p(t,\vec{x}) + \sigma(\vec{x})c(\vec{x})\nabla\cdot\vec{v}(t,\vec{x}) = 0, \quad t>0,\ \vec{x}\in\mathbb{R}^3.$$

Medium modeled by acoustic impedance $\sigma(\vec{x})$ & wave speed $c(\vec{x})$.

- **Electromagnetics:** electric field $\vec{E}(t,\vec{x})$ satisfies

$$\nabla\times\nabla\times\vec{E}(t,\vec{x}) + \frac{1}{c^2(\vec{x})}\partial_t^2\vec{E}(t,\vec{x}) = \vec{F}(t,\vec{x}), \quad t>0,\ \vec{x}\in\mathbb{R}^3,$$

for constant magnetic permeability and wave speed $c(\vec{x})$.

- $\vec{F}(t,\vec{x})$ models the excitation (localized at support of sensors) for $t>0$. Homogeneous initial conditions.

Inversion data are measurements of $p(t,\vec{x}_r)$ or $\vec{E}(t,\vec{x}_r)$ at the locations $\vec{x}_r$ of the receiving sensors.

Inverse problem

- **Inversion model** uses separation of scales:

$$\frac{1}{c^2(\vec{x})} = \frac{1}{c_o^2(\vec{x})}[1 + \rho(\vec{x}) + \mu(\vec{x})]$$

$c_o(\vec{x})$ = smooth, determines kinematics of waves (travel times).

$\rho(\vec{x})$ = rough part, is the reflectivity that we wish to determine.

$\mu(\vec{x})$ models small variations at small scale (clutter), that may have a cumulative scattering effect on the wave.

- **What can we estimate?**

- Smooth $c_o(\vec{x})$ (velocity analysis) with travel time tomography (many applied papers, theory of Uhlmann, Stefanov, Vasy) or using differential semblance optimization (Symes).

- Reflectivity ρ (imaging problem).

- Clutter cannot be estimated $\rightsquigarrow$ random model of uncertain μ.

Basic imaging uses single scattering approximation

$$D(t, \vec{\boldsymbol{x}}_r, \vec{\boldsymbol{x}}_s) \approx \int d\vec{\boldsymbol{y}}\, \rho(\vec{\boldsymbol{y}}) \alpha(\vec{\boldsymbol{x}}_s, \vec{\boldsymbol{y}}, \vec{\boldsymbol{x}}_r) f''[t - \tau(\vec{\boldsymbol{x}}_s, \vec{\boldsymbol{y}}, \vec{\boldsymbol{x}}_r)]$$

for smooth $\alpha(\vec{\boldsymbol{x}}_s, \vec{\boldsymbol{y}}, \vec{\boldsymbol{x}}_r)$ (geometrical spread), $\tau =$ travel time.

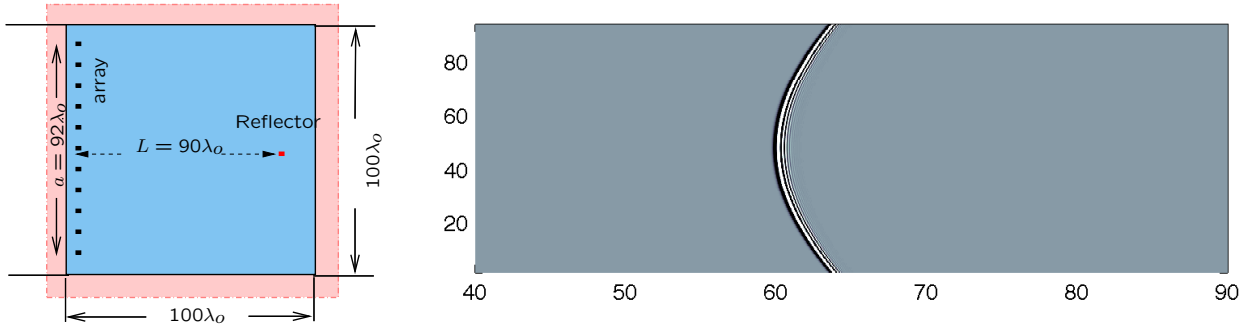

Scattered wave* by point reflector plotted vs. time on abscissa and receiver location on ordinate. Center sensor emits pulse $f(t)$.

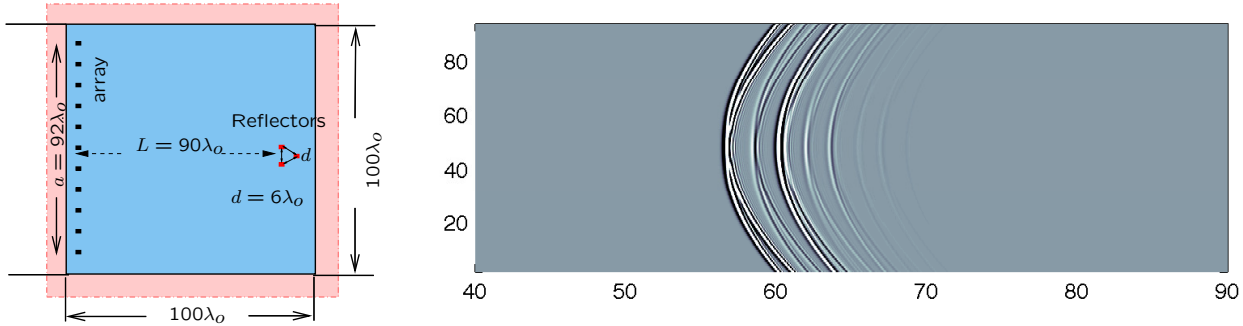

Multiply scattered echos among point reflectors are ignored.

*Numerical simulations by Chrysoula Tsogka.

Image formation - Reverse time (Kirchhoff) migration

- The imaging function

$$\mathcal{I}(\vec{\boldsymbol{y}}) = \sum_{r=1}^{N_r} \sum_{s=1}^{N_s} D\Big(\tau(\vec{\boldsymbol{x}}_s, \vec{\boldsymbol{y}}, \vec{\boldsymbol{x}}_r), \vec{\boldsymbol{x}}_r, \vec{\boldsymbol{x}}_s\Big)$$

is expected to peak at points $\vec{\boldsymbol{y}}$ in support of the reflectivity.

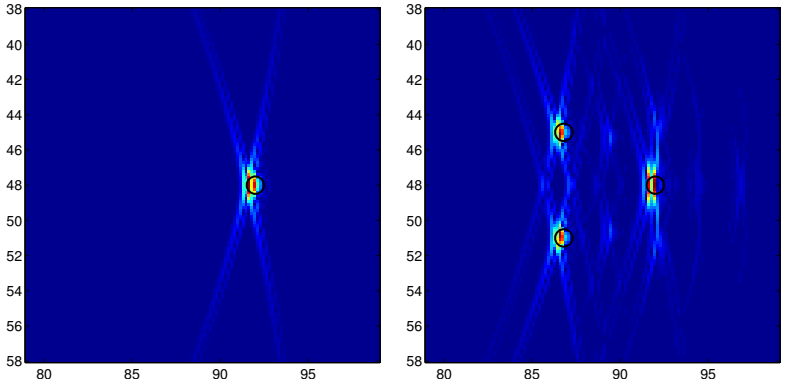

- Resolution in direction of propagation (range) depends on support of pulse (which is inverse proportional to the bandwdith).

- Resolution in cross-range is determined by typical wavelength, the aperture of the array and the distance (range) of scatterers.

Superresolution and uncertainty

• **Improved resolution** can be achieved by

- Use very broadand signals, like narrow pulses modulated at high frequency, as well as large (possibly synthetic) apertures.

- If image is "sparse" use optimization methods like ℓ_1 (Candès, Tao; Donoho, Elad; Fannjiang; Papanicolaou, Moscoso...) or subspace projection methods like MUSIC (Devaney and many engineering refs.). These are typically for single frequency waves.

• **Uncertainty impedes imaging:**

- Additive noise (easiest to mitigate).

- Multiple scattering (nonlinear) effects, specially those due to numerous inhomogeneities (clutter) are harder to deal with (e.g., atmosphere effects on X-band radar systems).

Noise vs. clutter effects in migration imaging*

Noise

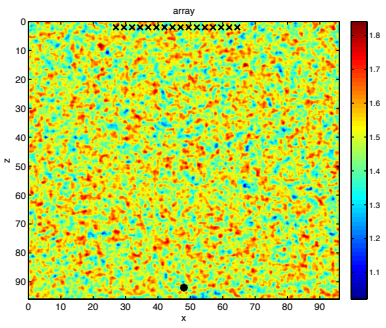

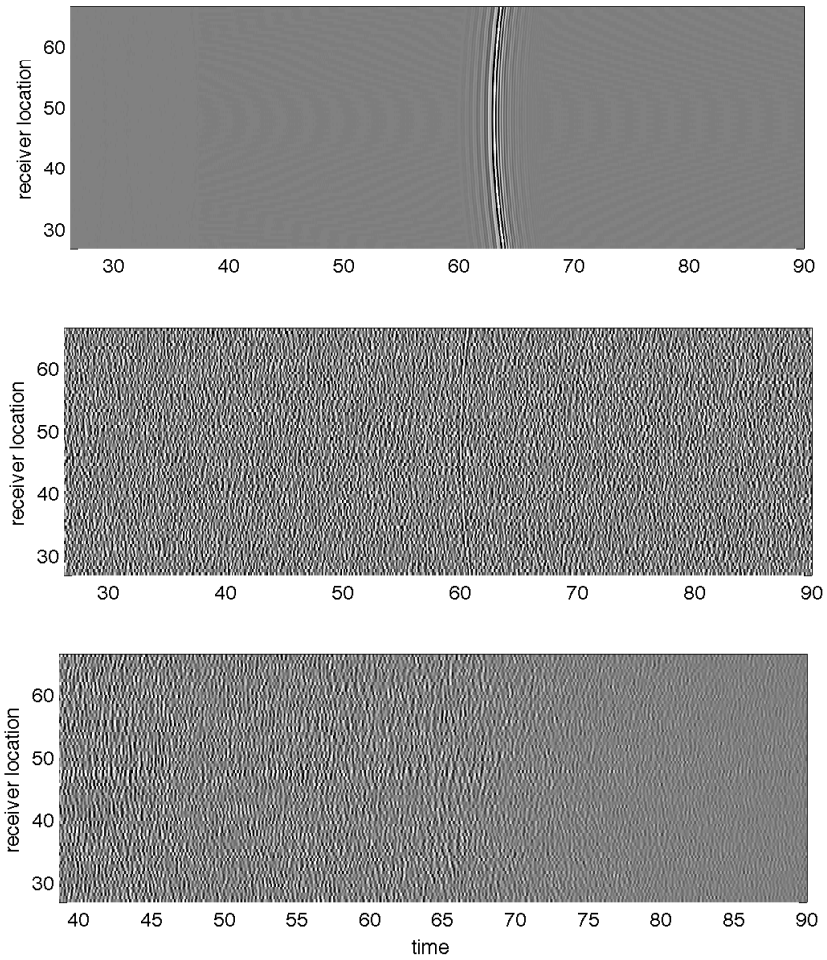

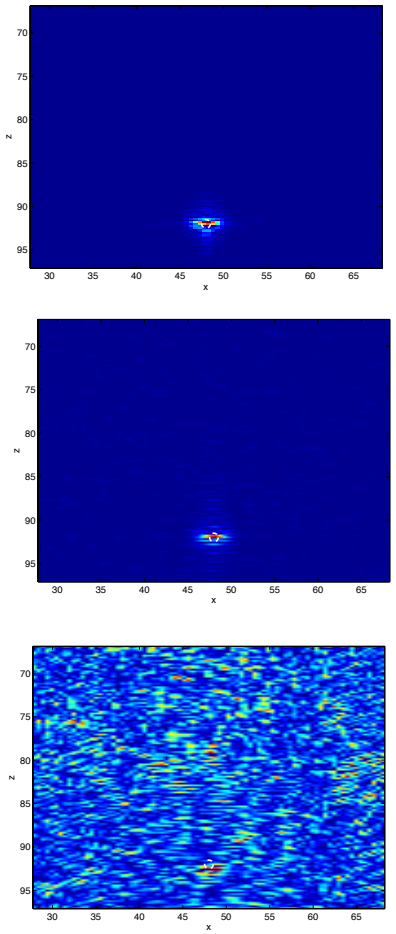

Noise is averaged out by summation (over large aperture).

*Simulations by Chrysoula Tsogka.

Super-resolution with time harmonic waves?

B., Josselin Garnier: Imaging P scatterers of diameter $\alpha\lambda$, $\alpha \ll 1$:

• Ammari: Electric field at $\vec{\boldsymbol{x}}_r$ due to point dipole source at $\vec{\boldsymbol{x}}_s$, with current $\vec{\boldsymbol{e}}_q$, for $1 \leq r, s \leq N$ and $1 \leq q \leq 3$,

$$\vec{\boldsymbol{E}}_q(\vec{\boldsymbol{x}}_r; \vec{\boldsymbol{x}}_s) = \sum_{p=1}^{P} \mathbf{G}(\vec{\boldsymbol{x}}_r, \vec{\boldsymbol{y}}_p) \boldsymbol{\rho}_p \mathbf{G}(\vec{\boldsymbol{y}}_p, \vec{\boldsymbol{x}}_s) \vec{\boldsymbol{e}}_q + O(\alpha^4).$$

Scatterers at $\vec{\boldsymbol{y}}_p$ with polarization tensors $\boldsymbol{\rho}_p \in \mathbb{C}^{3\times 3}$, $P \ll N$, $k = 2\pi/\lambda$ and $\mathbf{G}(\vec{\boldsymbol{x}}, \vec{\boldsymbol{y}}) = \left(\mathbf{I} + \frac{\nabla\nabla^T}{k^2}\right) \frac{e^{ik|\vec{\boldsymbol{x}}-\vec{\boldsymbol{y}}|}}{4\pi|\vec{\boldsymbol{x}}-\vec{\boldsymbol{y}}|}$.

• Noisy data model $\boldsymbol{D}_{\mathbf{W}} = \boldsymbol{D} + \boldsymbol{W}$,

$$\boldsymbol{D} = \sum_{p=1}^{P} \boldsymbol{\mathcal{G}}(\vec{\boldsymbol{y}}_p) \boldsymbol{\rho}_p \boldsymbol{\mathcal{G}}^T(\vec{\boldsymbol{y}}_p), \quad \boldsymbol{\mathcal{G}}(\vec{\boldsymbol{y}}_p) = \begin{pmatrix} \mathbf{G}(\vec{\boldsymbol{x}}_1; \vec{\boldsymbol{y}}_p) \\ \vdots \\ \mathbf{G}(\vec{\boldsymbol{x}}_N; \vec{\boldsymbol{y}}_p) \end{pmatrix} \in \mathbb{C}^{3N\times 3}$$

Complex Gaussian noise $\boldsymbol{W}$ with mean zero, independent entries with std $\mathfrak{S}$. (Noise with known correlation can be handled.)

MUSIC imaging with noisy data

• The $3N \times 3N$ matrix $\boldsymbol{D} = \sum_{p=1}^{P} \boldsymbol{\mathcal{G}}(\vec{\boldsymbol{y}}_p)\boldsymbol{\rho}_p\boldsymbol{\mathcal{G}}^T(\vec{\boldsymbol{y}}_p)$ has generically rank $3P \ll 3N$, with left singular vectors $\boldsymbol{u}_1, \ldots, \boldsymbol{u}_{3P}$.

• MUSIC imaging: Leading left singular vector $\boldsymbol{h}_1(\vec{\boldsymbol{y}})$ of $3N \times 3$ matrix $\boldsymbol{\mathcal{G}}(\vec{\boldsymbol{y}})$ satisfies

$$\boldsymbol{h}_1(\vec{\boldsymbol{y}}) \in \text{range}\, \boldsymbol{D} = \text{span}\{\boldsymbol{u}_1, \ldots, \boldsymbol{u}_{3P}\} \text{ iff } \vec{\boldsymbol{y}} \in \{\vec{\boldsymbol{y}}_1, \ldots, \vec{\boldsymbol{y}}_P\}.$$

• Noisy data matrix $D_{\mathbf{W}}$ has r significant singular values $\tilde{\sigma}_j \geq 2\mathfrak{S}$ and left singular vectors $\tilde{\boldsymbol{u}}_j$, where $\mathfrak{S}$ can be estimated.

Random matrix theory asymptotic results*: $\left|\tilde{\boldsymbol{u}}_j^{\star}\boldsymbol{u}_q\right|^2 \approx \delta_{jq}\cos^2\theta_j$

$$\cos^2\theta_j = 1 - \left(\frac{\mathfrak{S}}{\sigma_j}\right)^2, \quad \sigma_j \approx \frac{1}{2}\left[\tilde{\sigma}_j + \sqrt{\tilde{\sigma}_j^2 - (2\mathfrak{S})^2}\right].$$

*Benaych-Georges, Guionnet, Maida

MUSIC imaging with noisy data

- Scatterer locations are estimated by peaks of

$$\mathcal{I}(\vec{\boldsymbol{y}}) = \left[1 - \sum_{j=1}^{r} \frac{|\widetilde{\boldsymbol{u}}_j^{\star} \boldsymbol{h}_1(\vec{\boldsymbol{y}})|^2}{\cos^2 \theta_j} \right]^{-1}$$

- Once we know the locations, can also estimate the reflectivity (polarization) tensors $\boldsymbol{\rho}_p$.

- Smaller size of the array aperture relative to range of scatterers and incomplete measurements lower effective rank: $r < 3P \rightsquigarrow$ worse resolution and $\boldsymbol{\rho}_p$ estimates.

Numerical simulations

Images with planar square array of aperture 10 wavelengths and $N = 441$ antennas. Noise is stronger than signal (SNR = 0.03).

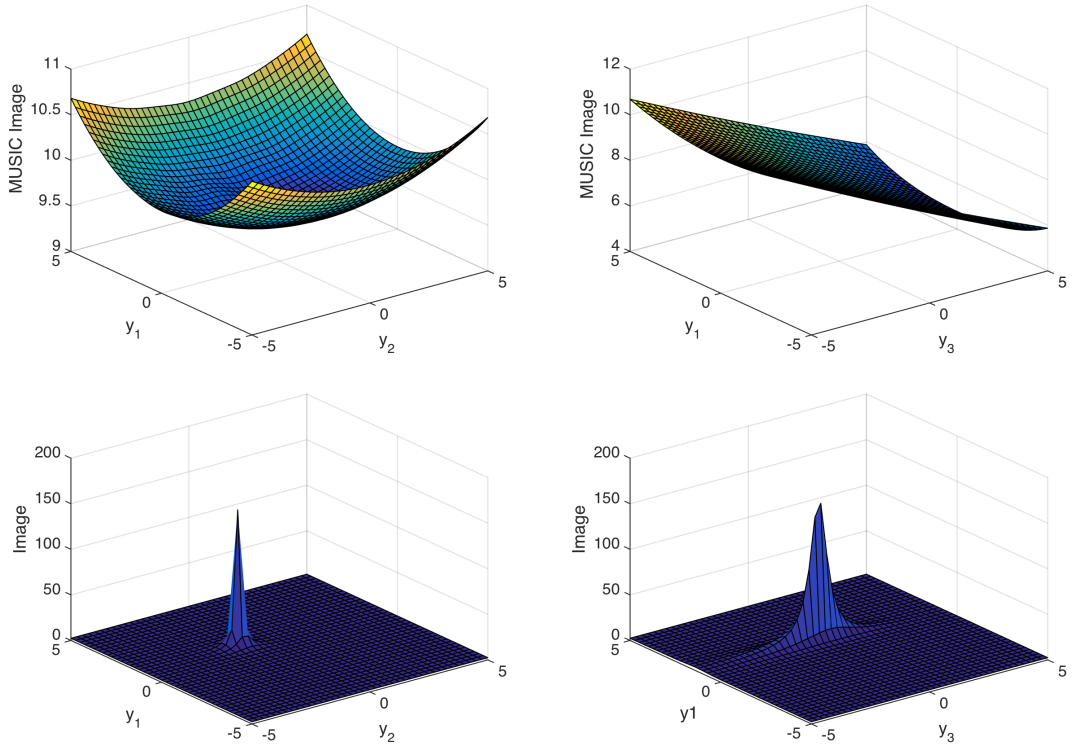

Imaging of three scatterers

Large aperture

Small aperture

SNR = 0.03

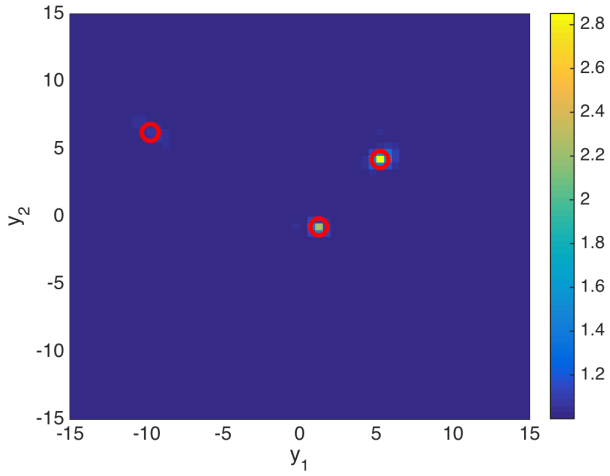

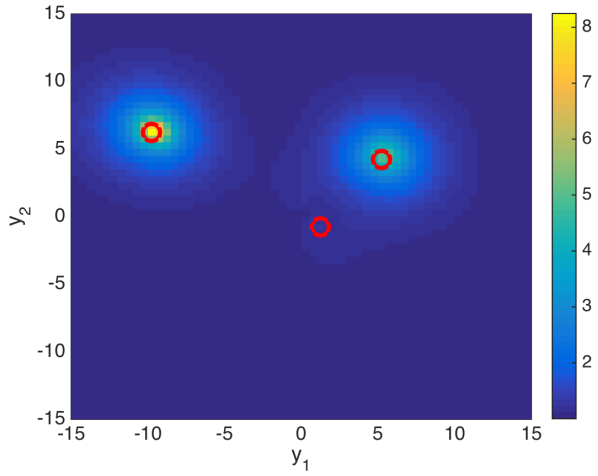

SNR = 0.1

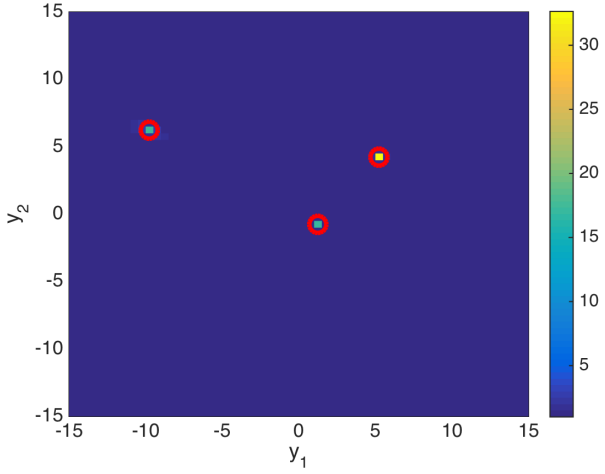

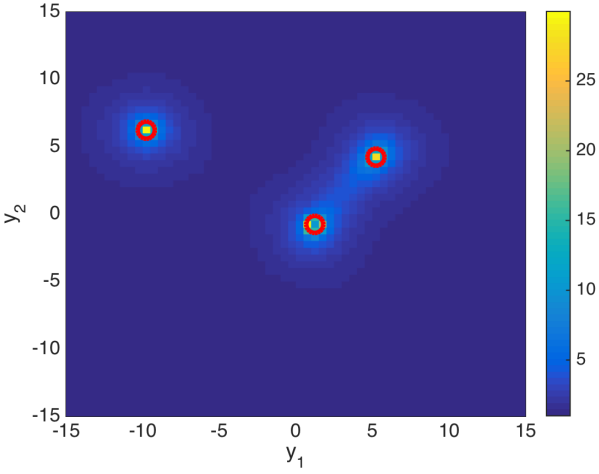

Conclusion: noise can be mitigated.

Clutter viewed as a realization of random process $\mu(\vec{x})$

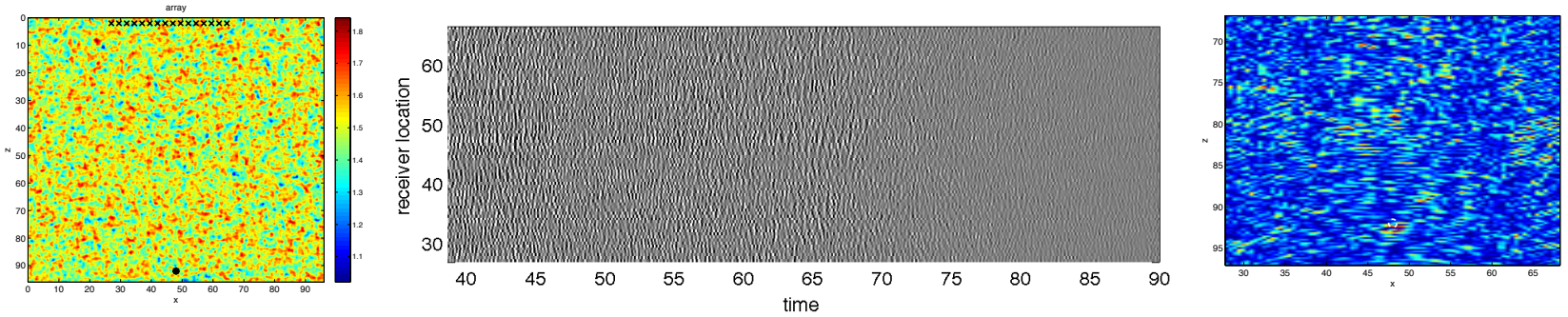

• Due to cumulative scattering neither $p(t, \vec{\boldsymbol{x}})$ nor its expectation $\mathbb{E}[p(t, \vec{\boldsymbol{x}})]$ are close to the model $p_o(t, \vec{\boldsymbol{x}})$ that neglects the clutter.

• The coherent field $\mathbb{E}[p(t, \vec{\boldsymbol{x}})]$ decays with the distance of propagation in the medium $\rightsquigarrow$ random fluctuations gain strength.

• Coherent Interferometric Imaging (CINT) (B., Garnier, Papanicolaou and Tsogka) uses cross-correlations of the measurements to mitigate random effects. It images with energy resolved over direction and time of arrival (Wigner transform).

Illustration: Sonar with random geometrical optics model

• For weak inhomogeneities and wavelengths $\ll$ correlation length in random medium $\ll$ distance of propagation,

$$D(t,\vec{\boldsymbol{x}}_r,\vec{\boldsymbol{x}}_s) \approx \int \frac{d\omega}{2\pi} e^{-i\omega t}\hat{f}(\omega) \sum_{p=1}^{P} \rho_p\, \hat{G}(\omega,\vec{\boldsymbol{x}}_r,\vec{\boldsymbol{y}}_p)\hat{G}(\omega,\vec{\boldsymbol{y}}_p,\vec{\boldsymbol{x}}_s)$$

with $\hat{G}(\omega,\vec{\boldsymbol{x}},\vec{\boldsymbol{y}}_p) = \frac{e^{i\omega[\tau(\vec{\boldsymbol{x}},\vec{\boldsymbol{y}}_p)+\delta\tau(\vec{\boldsymbol{x}},\vec{\boldsymbol{y}}_p)]}}{4\pi|\vec{\boldsymbol{x}}-\vec{\boldsymbol{y}}_p|}$.

• Random travel times $\delta\tau(\vec{\boldsymbol{x}},\vec{\boldsymbol{y}}_p)$ are Gaussian distributed, with large std $\rightsquigarrow \mathbb{E}[D(t,\vec{\boldsymbol{x}}_r,\vec{\boldsymbol{x}}_s)] \approx 0$.

• In cross-correlations for nearby receivers and sources

$$\int dt'\, D(t',\vec{\boldsymbol{x}}_{r'},\vec{\boldsymbol{x}}_{s'})\overline{D(t'-t,\vec{\boldsymbol{x}}_r,\vec{\boldsymbol{x}}_s)} = \int \frac{d\omega}{2\pi}\, e^{-i\omega t}\hat{D}(\omega,\vec{\boldsymbol{x}}_{r'},\vec{\boldsymbol{x}}_{s'})\overline{\hat{D}(\omega,\vec{\boldsymbol{x}}_r,\vec{\boldsymbol{x}}_s)}$$

random phases are reduced $\rightsquigarrow$ coherence enhancement.

• Superposition of cross-correlations evaluated at the proper travel time $\rightsquigarrow$ robust CINT image with respect to realization of random medium. But clutter manifests in blurrier images.

Super-resolution in random media?

B. and Ilker Kocyigit: Deblur CINT image:

For sufficiently large planar aperture a and bandwidth B,

$$\mathcal{I}(\vec{\boldsymbol{y}}) \approx \sum_{p,q=1}^{P} \rho_p \overline{\rho_q}\, \mathfrak{M}(\vec{\boldsymbol{y}}, \vec{\boldsymbol{y}}_p, \vec{\boldsymbol{y}}_q)\, e^{-\frac{\left|\boldsymbol{y}-\frac{\boldsymbol{y}_p+\boldsymbol{y}_q}{2}\right|^2}{2R^2} - \frac{\left|z-\frac{z_p+z_q}{2}\right|^2}{2R_z^2}}, \qquad \vec{\boldsymbol{y}} = (\boldsymbol{y}, z).$$

• CINT resolution $R = \lambda_o L/X_d$ and $R_z = c_o/\Omega_d$ in terms of decorrelation length $X_d \ll a$ and frequency $\Omega_d \ll B$ of waves at array.

• $\mathfrak{M}(\vec{\boldsymbol{y}}, \vec{\boldsymbol{y}}_p, \vec{\boldsymbol{y}}_q)$ decays very rapidly in $\|\vec{\boldsymbol{y}}_p - \vec{\boldsymbol{y}}_q\| \rightsquigarrow$ basically a diagonal (convolution) kernel.

Unknown $|\rho_p|^2$ and can be extracted with convex optimization*.

*Candès, Fernandez-Granda; Castro, Gamboa; Demanet; Peyré, ...

Numerical results. Typical cross-range localization.

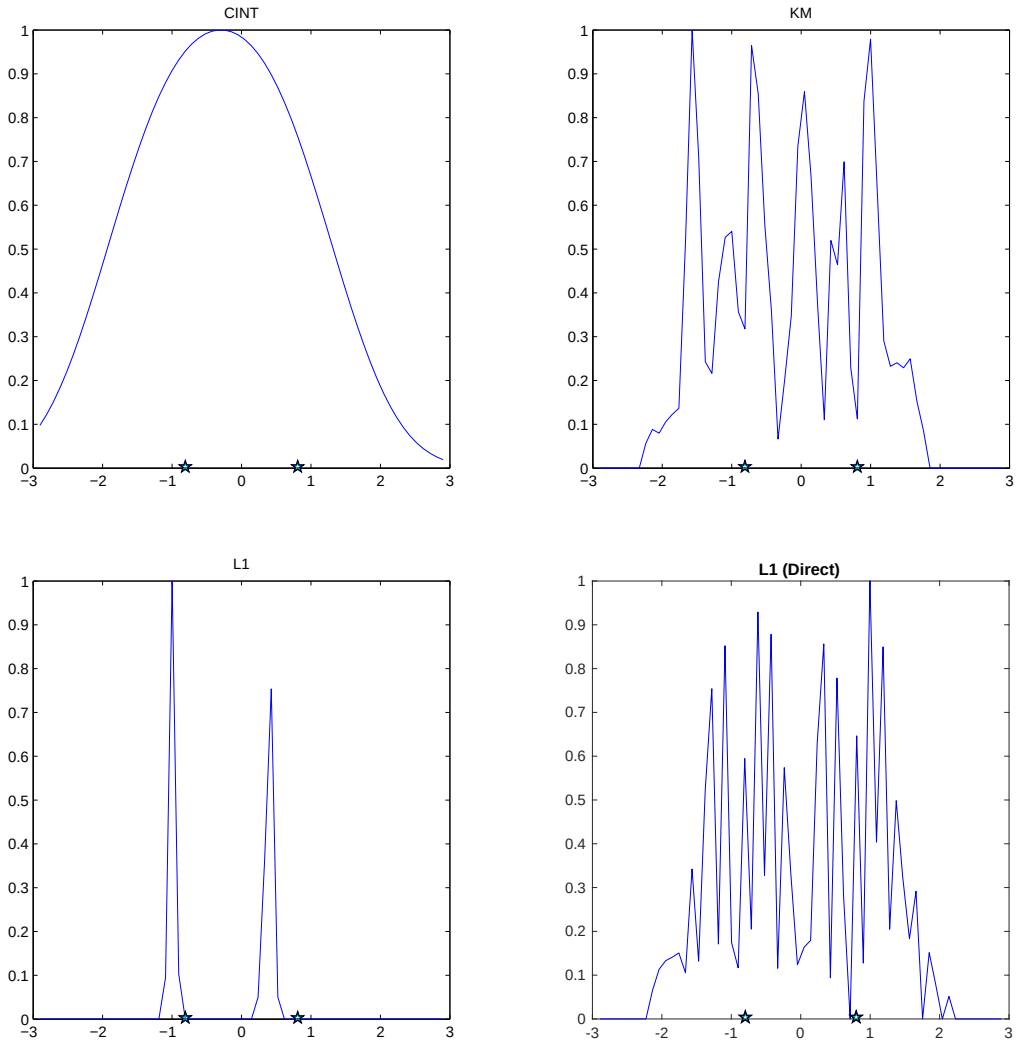

Abscissa is in $R = \lambda_o L/X_d$ units. Direct ℓ_1 means minimize $\|\rho\|_1$ constrained by fitting array data within a tolerance.

Filters of multiple scattering effects

• For imaging small reflectors in strong random media (B., Cueto, Papanicolaou, Tsogka; Aubry, Derode) using signal processing, computational harmonic analysis and random matrix theory.

• Reverberations between sought reflectors may also be strong*

$c(\vec{x})$

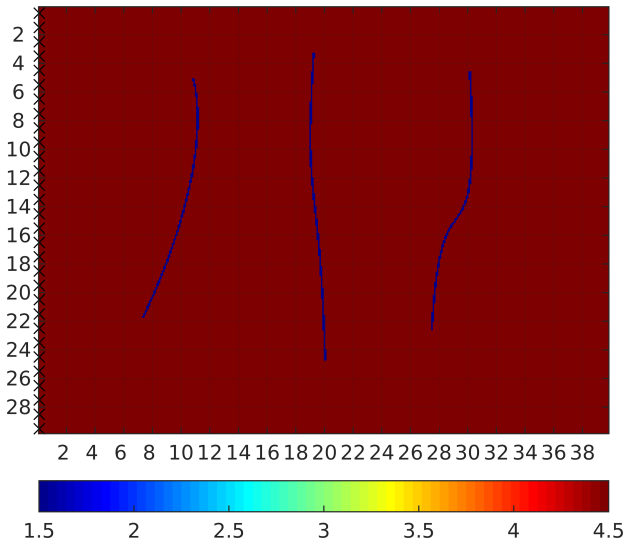

Migration image

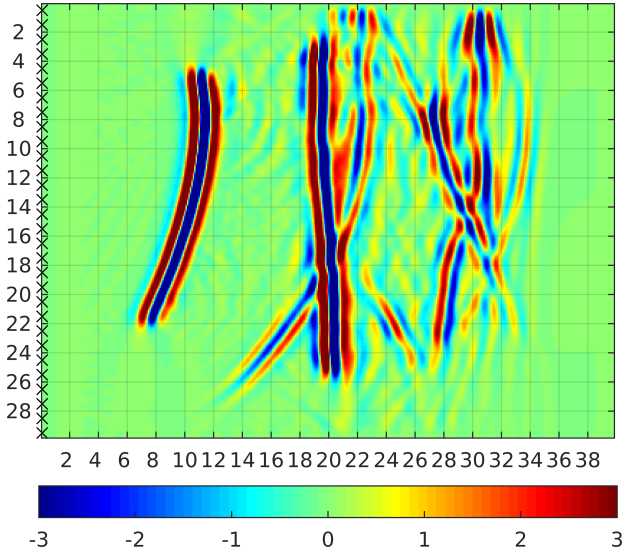

B. and Druskin, Mamonov, Zaslavsky: use data-driven reduced order models to transform the measurements to those corresponding to single scattering.

*Results by Druskin, Mamonov, Zaslavsky.

Setup for data-driven reduced order model

- Assume known c_o. Unknown is acoustic impedance $\sigma(\vec{x})$.

Explanation in 1-D for $x \in (0, X)$. Sound hard boundary at $x = 0$ i.e., $v(t, 0) = 0$ and sound soft at $x = X$ i.e., $p(t, X) = 0$.

- After some manipulations and for pulse $f(t)$ with non-negative Fourier transform, can restate acoustic wave system as

$$\partial_t \begin{pmatrix} P(t,x) \\ V(t,x) \end{pmatrix} = \begin{pmatrix} 0 & -\mathcal{L}_q \\ \mathcal{L}_q^T & 0 \end{pmatrix} \begin{pmatrix} P(t,x) \\ V(t,x) \end{pmatrix}, \quad t > 0, \quad 0 < x < X,$$

where

$$P(t,x) = p(t,x)/\sqrt{\sigma(x)}, \quad V(t,x) = -\sqrt{\sigma(x)} v(t,x).$$

- Excitation in initial condition $P(0, x) = b(x)$, $V(0, x) = 0$, with $b(x)$ supported on sensor at $x = 0^+$.

- Operator* $\mathcal{L}_q = -c_o \partial_x + \frac{c_o}{2} \partial_x q(x)$ is linear in $q(x) = \ln \sigma(x)$.

*Discretization on very fine grid with N points, $\mathcal{L}_q$ is bidiagonal matrix.

Data-driven reduced order model (ROM)

- Pressure field at time* $j\tau$

$$\boldsymbol{P}_j = \cos\left(j\tau\sqrt{\mathcal{L}_q\mathcal{L}_q^T}\right)\boldsymbol{b} = T_j(\mathcal{P})\boldsymbol{b}, \quad \mathcal{P} = \cos\left(\tau\sqrt{\mathcal{L}_q\mathcal{L}_q^T}\right),$$

where $T_j =$ Chebyshev polynomial of first kind.

- Data are: $D_j = \boldsymbol{b}^T\boldsymbol{P}_j = \boldsymbol{b}^T T_j(\mathcal{P})\boldsymbol{b}$.

- ROM $n \times n$ matrix $\tilde{\mathcal{P}}$ satisfying

$$D_j = \tilde{\boldsymbol{b}}^T T_j(\tilde{\mathcal{P}})\tilde{\boldsymbol{b}}, \quad j = 0, \ldots, 2n-1, \quad \tilde{\boldsymbol{b}} = D_0^{1/2}\boldsymbol{e}_1,$$

is the projection of $\mathcal{P}$ on span $\{\boldsymbol{P}_0, \ldots, \boldsymbol{P}_{n-1}\}$,

$$\tilde{\mathcal{P}} = \boldsymbol{Q}^T\mathcal{P}\boldsymbol{Q}, \qquad \mathbf{P} = (\boldsymbol{P}_0, \ldots, \boldsymbol{P}_{n-1}) = \boldsymbol{Q}\boldsymbol{R}.$$

*Time sampling consistent with Nyquist rate.

Causal construction: $\mathrm{P} = (P_0, \ldots, P_{n-1}) = QR$

Causality $\rightsquigarrow$ Q is concentrated near the diagonal and is almost independent of q. Moreover, $\tilde{\mathcal{P}}$ is tridiagonal.

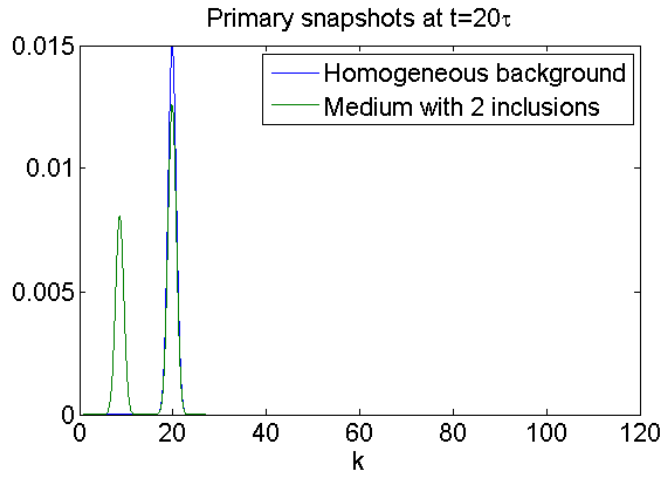

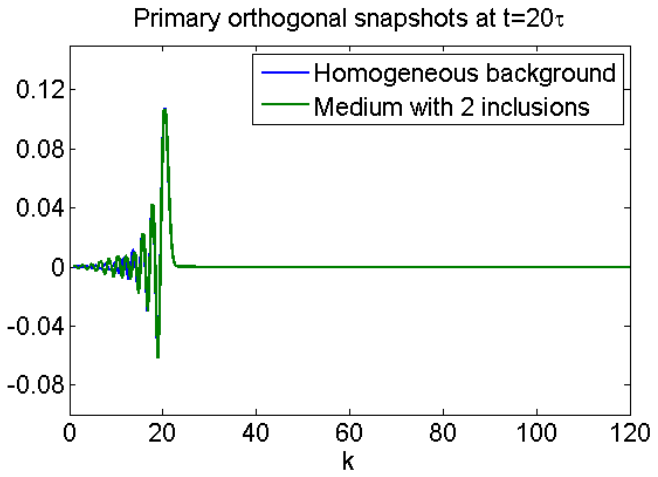

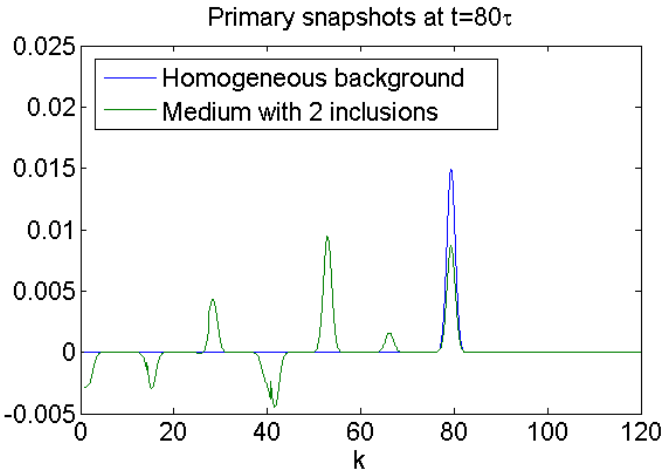

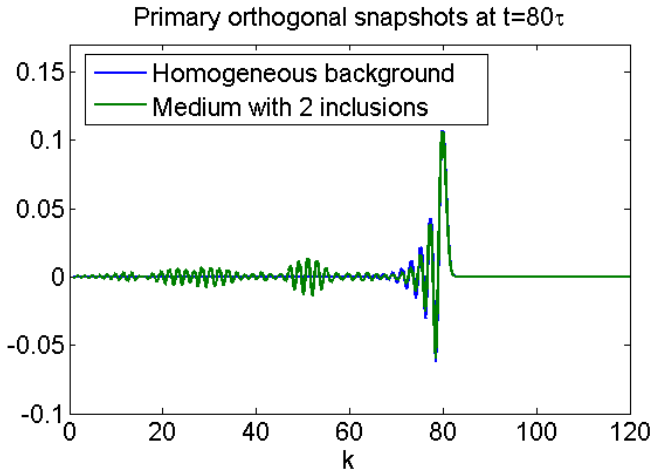

Columns of P on left and of Q on right.

From data to ROM

- Start with $\mathrm{P} = (\boldsymbol{P}_0, \ldots, \boldsymbol{P}_{n-1}) = \boldsymbol{Q}\boldsymbol{R}$ and use $\boldsymbol{P}_j = T_j(\mathcal{P})\boldsymbol{b}$

$$
\begin{aligned}
(\mathrm{P}^T\mathrm{P})_{jk} &= \boldsymbol{b}^T T_j(\mathcal{P}) T_k(\mathcal{P})\boldsymbol{b} \\
&= \frac{1}{2}\boldsymbol{b}^T\Big[T_{j+k}(\mathcal{P}) + T_{|j-k|}(\mathcal{P})\Big]\boldsymbol{b} \\
&= \frac{1}{2}\Big(D_{j+k} + D_{|j-k|}\Big) = (\boldsymbol{R}^T\boldsymbol{R})_{jk}, \quad 0 \le j,k \le n-1.
\end{aligned}
$$

Thus, $\boldsymbol{R}$ can be computed by Cholesky decomposition.

- ROM $\tilde{\mathcal{P}} = \boldsymbol{Q}^T\mathcal{P}\boldsymbol{Q} = \boldsymbol{R}^{-T}\Big(\mathrm{P}^T\mathcal{P}\mathrm{P}\Big)\boldsymbol{R}^{-1}$ can be computed from

$$
\begin{aligned}
\Big(\mathrm{P}^T\mathcal{P}\mathrm{P}\Big)_{j,k} &= \boldsymbol{b}^T T_j(\mathcal{P})\mathcal{P}T_k(\mathcal{P})\boldsymbol{b} \\
&= \frac{1}{4}\Big(D_{j+k+1} + D_{|k-j+1|} + D_{|k-j-1|} + D_{|k+j-1|}\Big).
\end{aligned}
$$

Propagator factorization

- We show that

$$\tilde{\mathcal{P}} = \boldsymbol{Q}^T \mathcal{P} \boldsymbol{Q} = \boldsymbol{Q}^T \cos\left(\tau \sqrt{\mathcal{L}_q \mathcal{L}_q^T}\right) \boldsymbol{Q} = \boldsymbol{I}_n - \frac{\tau^2}{2} \tilde{\mathcal{L}}_q \tilde{\mathcal{L}}_q^T, \quad \tilde{\mathcal{L}}_q = \boldsymbol{Q}^T \mathcal{L}_q \boldsymbol{Q}_V$$

where $\boldsymbol{Q}_V$ is the projection matrix on space spanned by the velocity snapshots $\boldsymbol{V}_j$, for $j = 0, \ldots, n-1$.

- $\tilde{\mathcal{P}}$ is $n \times n$ tridiagonal, so Cholesky factor $\tilde{\mathcal{L}}_q$ is bidiagonal. It is the projection of $N \times N$ matrix $\mathcal{L}_q =$ fine grid discretization of $-c_o \partial_x + \frac{c_o}{2} \partial_x q(x)$.

- Projection matrices $\boldsymbol{Q}$ and $\boldsymbol{Q}_V$ are approx. independent of q.

$\rightsquigarrow$ $\tilde{\mathcal{L}}_q$ is approximately linear in q.

Data to Born (single scattering) mapping

• The single scattering (Born) approximation applies to small $q^\epsilon = \epsilon q$, where $\epsilon \ll 1$.

• Because $\tilde{\mathcal{L}}_q$ is approximately linear in q, we can calculate

$$\tilde{\mathcal{L}}_{q^\epsilon} = \tilde{\mathcal{L}}_0 + \epsilon\big(\tilde{\mathcal{L}}_q - \tilde{\mathcal{L}}_0\big),$$

and obtain the transformed data

$$D_j^\epsilon = \tilde{\boldsymbol{b}}^T T_j(\tilde{\boldsymbol{\mathcal{P}}}^\epsilon)\tilde{\boldsymbol{b}}, \quad j = 0, \ldots, 2n-1,$$

where

$$\tilde{\boldsymbol{\mathcal{P}}}^\epsilon := \boldsymbol{I}_n - \frac{\tau^2}{2}\tilde{\mathcal{L}}_{q^\epsilon}\tilde{\mathcal{L}}_{q^\epsilon}^T.$$

• Everything generalizes to higher dimensions, where the basic difference is that we work with block tridiagonal $\tilde{\boldsymbol{\mathcal{P}}}$.

Numerical results in 1-D

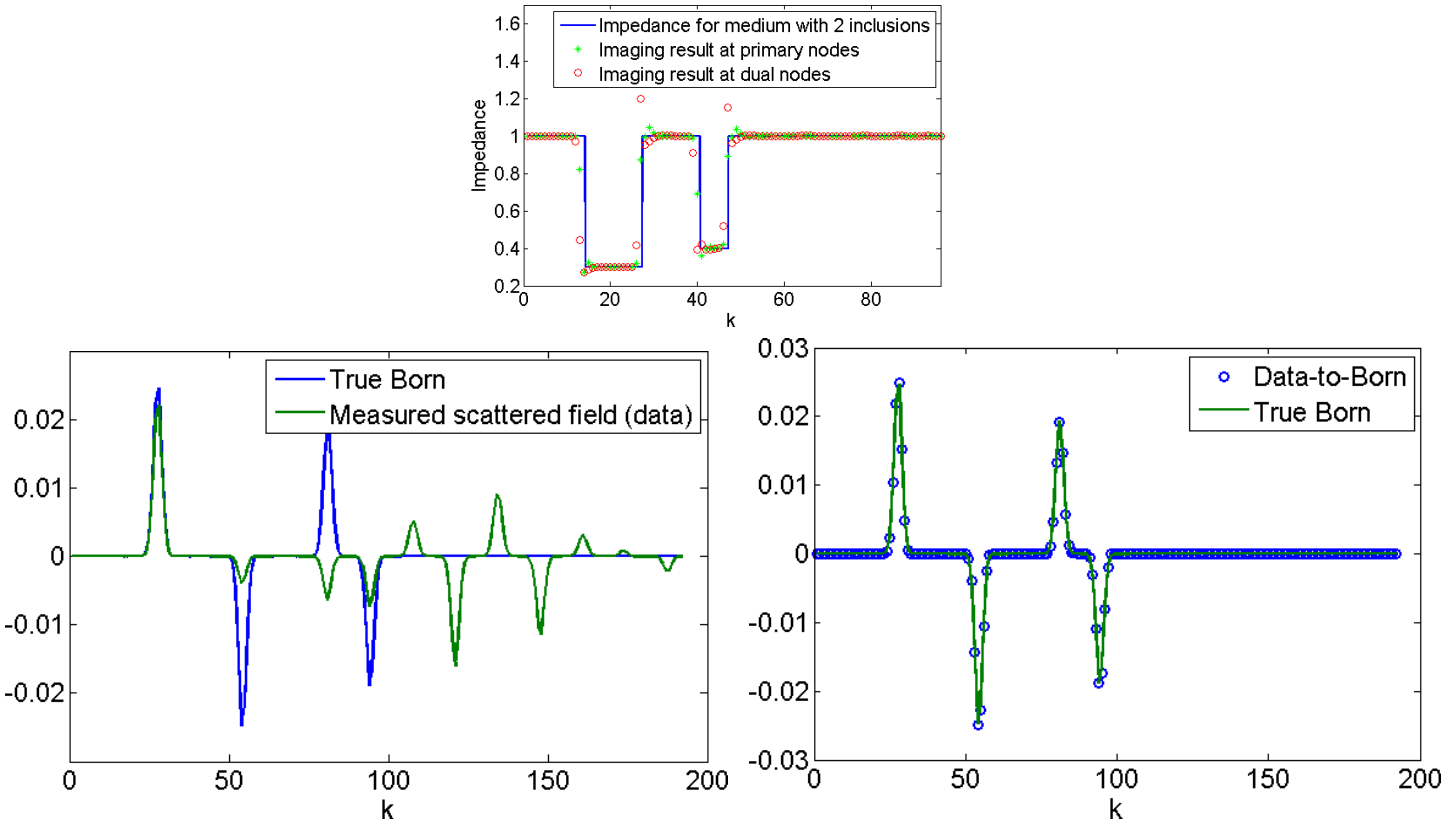

Numerical results in 2-D

$\sigma(\boldsymbol{x})$

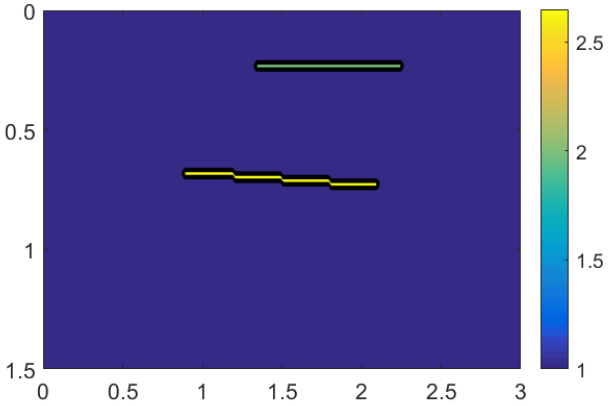

$c_O(\boldsymbol{x})$

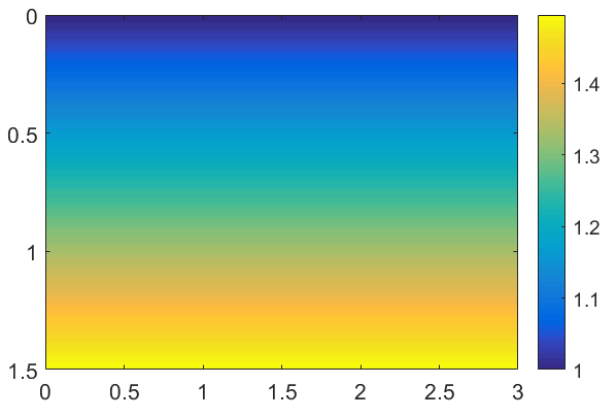

Scattered data

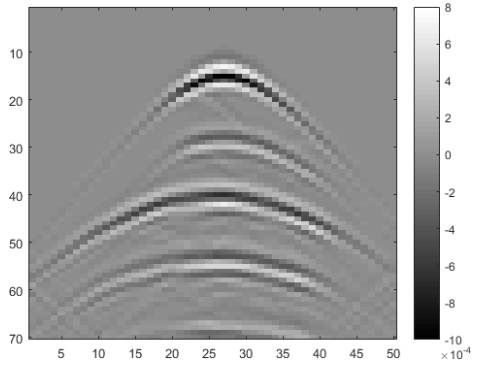

Born approximation

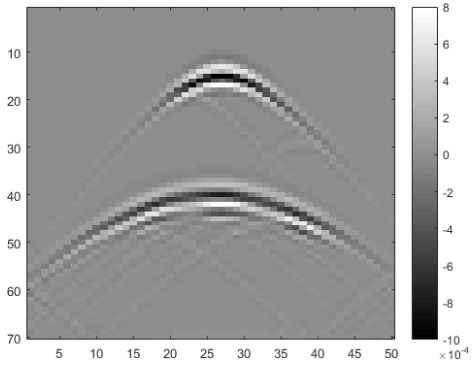

DtB

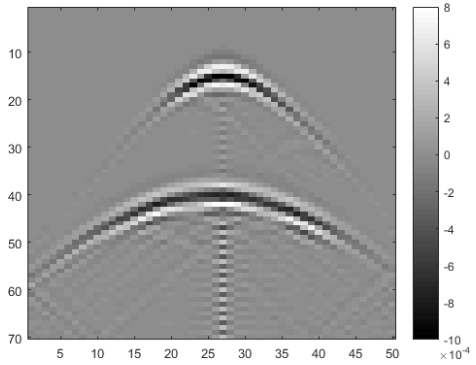

Acknowledgements

- The results presented are in collaboration with:

Josselin Garnier (Ecole Polytechnique), Vladimir Druskin and Mike Zaslavsky (Schlumberger-Doll), Ilker Kocyigit (Michigan), Alexander Mamonov (Houston), George Papanicolaou (Stanford), Chrysoula Tsogka (Crete).

- Thank you for support:

Dr. Arje Nachman (AFOSR)
Dr. Lora Billings (NSF)
Dr. Reza Malek-Madani and Dr. Wen Masters (ONR).